

Search for Gamma-Ray Burst Classes with the RHESSI Satellite

J. Řípa¹, A. Mészáros¹, C. Wigger^{2,4}, D. Huja¹, R. Hudec³, and W. Hajdas²

¹ Charles University, Faculty of Mathematics and Physics, Astronomical Institute, V Holešovičkách 2, CZ 180 00 Prague 8, Czech Republic

e-mail: ripa@sirrah.troja.mff.cuni.cz

e-mail: meszaros@cesnet.cz

e-mail: David.HUJA@seznam.cz

² Paul Scherrer Institute, CH-5232 Villigen, Switzerland

e-mail: wojtek.hajdas@psi.ch

e-mail: claudia.wigger@kanti-wohlen.ch

³ Astronomical Institute, Academy of Sciences of the Czech Republic, CZ 251 65 Ondřejov, Czech Republic

e-mail: rhudec@asu.cas.cz

⁴ Kantonsschule Wohlen, 5610 Wohlen, Switzerland

Received September 04, 2008; accepted February 02, 2009

ABSTRACT

Aims. A sample of 427 gamma-ray bursts (GRBs), measured by the RHESSI satellite, is studied statistically with respect to duration and hardness ratio.

Methods. Standard statistical tests are used, such as χ^2 , F-test and the maximum likelihood ratio test, in order to compare the number of GRB groups in the RHESSI database with that of the BATSE database.

Results. Previous studies based on the BATSE Catalog claim the existence of an intermediate GRB group, besides the long and short groups. Using only the GRB duration T_{90} as information and χ^2 or F-test, we have not found any statistically significant intermediate group in the RHESSI data. However, maximum likelihood ratio test reveals a significant intermediate group. Also using the 2-dimensional hardness / T_{90} plane, the maximum likelihood analysis reveals a significant intermediate group. Contrary to the BATSE database, the intermediate group in the RHESSI data-set is harder than the long one.

Conclusions. The existence of an intermediate group follows not only from the BATSE data-set, but also from the RHESSI one.

Key words. gamma-rays: bursts

1. Introduction

In the years 1991 – 2000 cca 3000 gamma-ray bursts (GRBs) were detected by the BATSE instrument on board the Compton Gamma-Ray Observatory (Meegan et al. 2001). After the end of this mission (June 2000) the number of discovered GRBs decreased (down to $\sim 100 - 200$ GRBs annually) due to different observational methods on the operating satellites. Any observational GRB database from the period 2000 and latter, can have a great importance. Such important GRB observations are records obtained by the RHESSI satellite (Holman et al. 2008) ~ 70 /year.

Originally it was found (Kouveliotou et al. 1993) that there exist two GRB classes: the short one with durations $\lesssim 2$ s and the long one with durations $\gtrsim 2$ s. This was confirmed with GRB data from the Konus-Wind instrument (Aptekar et al. 1998). However, some articles point to the existence of three classes of GRBs in the BATSE database with respect to their durations (Horváth 1998, Horváth 2002). The work Horváth et al. (2008), using maximum likelihood ratio test on durations, gives that there is a statistically significant intermediate group in the Swift data-set. Also Horváth et al. (2004) and Horváth et al. (2006) claimed that, when using a 2-dimensional plane of hardness ratio vs. duration, three classes of GRBs can be found

in the BATSE data-set. Mukherjee et al. (1998) pointed to the existence of three GRB classes in multiparameter space. In another multidimensional analysis of the BATSE catalog by Chattopadhyay et al. (2007) it is argued that at least three clusters of GRBs are found. Some articles also say that the third class (with intermediate duration), observed by BATSE, is a bias caused by an instrumental effect (Hakkila et al. 2000). In Hakkila et al. (2004) there is a review and discussion of GRB classifying, based on statistical clustering and data mining techniques, placing the intermediate group as a separate source population in doubt.

The purpose of this paper is to investigate the number of GRB groups in another data set, namely in the GRB data set provided by the RHESSI satellite. Although the main goal of the RHESSI satellite is the study of solar physics, it has a useful set of GRB observations also covering the period 2002 – 2004. Hence its study can be maximally useful. Trivially, any comparison of different catalogs using different instruments is useful for an independent confirmation of previous results.

In the first step the 1-dimensional duration distribution of GRBs observed by RHESSI is analysed, and in the second step the two-dimensional plane of hardness ratio vs. duration is used. In order to determine the number of GRB groups, standard statistical tests described in Trumpler & Weaver (1953), Press et al. (1992), Zey et al. (2006) are used.

The paper is organized as follows: in section 2, the RHESSI satellite and the analysed data-set are described. In section 3, we present the duration distribution for the RHESSI GRBs and its analysis. In section 4, the 2-dimensional hardness ratio vs. duration distribution and the maximum likelihood fit of these data are presented. In sections 5 and 6, the discussion and conclusion follow. At the end, the RHESSI data-sample is listed.

2. The RHESSI Data Sample

The Ramaty High Energy Solar Spectroscopic Imager (RHESSI) is a NASA Small Explorer satellite designed to study hard X-rays and gamma-rays from solar flares (Lin et al. 2002). It consists mainly of an imaging tube and a spectrometer. The spectrometer consists of nine germanium detectors (7.1 cm in diameter and a height of 8.5 cm) (Smith et al. 2002). They are only lightly shielded, thus making RHESSI also very useful to detect non-solar photons from any direction (Smith et al. 2003). The energy range for GRB detection extends from about 30 keV up to 17 MeV. Over a wide range of energies and GRB incoming directions, the effective area is around 150 cm² (Wigger et al. 2006b). With a field of view of about half of the sky, RHESSI observes about one or two GRBs per week. Photon hits are stored event-by-event in onboard memory with a time sampling of $\Delta t = 1 \mu\text{s}$ resolution. The energy resolution for lines is excellent: $\Delta E = 3 \text{ keV}$ at 1000 keV.

We used the RHESSI GRB Catalog (Wigger et al. 2008) and the Cosmic Burst List (Hurley 2008) to find 487 GRBs in the RHESSI data between the 14th February 2002 and 25th April 2008. We should mention the strategy how RHESSI GRBs are found. There is no automatic GRB search routine. Only if there is a message from any other instrument of the IPN (Hurley 2007), the RHESSI data are searched for a GRB signal. Therefore, in our data-set there are only GRBs, which are also observed by other instruments. The biggest overlap is with Konus-W. About 85 % of all RHESSI GRBs are also observed by Konus-W (Wigger et al. 2006a).

For a deeper analysis we have chosen a subset of 427 GRBs with a signal/noise ratio better than 6. We have used the SolarSoftWare (Freeland et al. 2008) program running under the Interactive Data Language (RSI IDL) programming application as well as our own IDL routines to derive count light-curves (with the time resolution better than 10 % of the burst's duration for the great majority of our whole data-set) and count fluences from the rear detectors' segments (except number R2) of the RHESSI spectrometer (Smith et al. 2002) in the energy band from 25 keV to 1.5 MeV. This data-set (together with the time resolutions of derived light-curves) are listed in the Table 7 – Table 13.

3. Duration Distribution

First we study the 1-dimensional duration distribution. We use T_{90} as the GRB duration, i.e. the time interval during which the cumulative counts increase from 5 % to 95 % above background (Meegan et al. 2001). The T_{90} uncertainty consists of two components. We make an assumption that one is given by the count fluence uncertainty during T_{90} (δt_s), which is given by Poisson noise, and the second one is the time resolution of derived light-curves (δt_{res}). The total T_{90} uncertainty δt was calculated as $\delta t = \sqrt{\delta t_s^2 + \delta t_{res}^2}$.

The histogram of the times T_{90} gives a distribution with two maxima: at approximately 0.2 s and 20 s (Fig. 1.). The histogram

consists of 19 equally wide bins on logarithmic scale (with base 10) starting at 0.09 s and ending at 273.4 s.

We follow the method done by Horváth (1998) and fitted one, two (Fig. 1.) and three (Fig. 2.) log-normal functions and used the χ^2 test to evaluate these fits. The minimal number of GRBs per bin is 4 (last bin), hence the use of the χ^2 test is possible.

In the case of the fit with one log-normal function we obtained $\chi^2 \approx 157$ for 17 degrees of freedom (dof). Therefore, this hypothesis is rejected on a smaller than 0.01 % significance level.

The fit with two log-normal functions is shown in Fig. 1 and the fit with three log-normal functions in Fig. 2. The parameters of the fits, the values of χ^2 , the degrees of freedom and the goodness-of-fits are listed in Table 1.

The assumption of two groups being represented by two log-normal fits is acceptable, the fit with three log-normal functions even more. The question is whether the improvement in χ^2 is statistically significant. To answer this question, we used the F-test, as described by Band et al. (1997), Appendix A. The F-test gives a probability of 6.9 % of the improvement in χ^2 being accidental. This value is remarkably low, but not low enough to reject the hypothesis that two log-normal functions are still enough to describe the observed duration distribution.

In order to know how the T_{90} uncertainties effect our result, we randomly picked up one half of the bursts and shifted their durations by the full amount of their uncertainties to lower values and the second half to higher values. Then we made a histogram and recalculated the best fitted parameters, χ^2 and F-test. The results for ten such calculations are listed in the Table 2. This method also gives us information how the fitted parameters vary, and thus tells what are their uncertainties. From Table 2 we see that, on average, the improvement in χ^2 is not significant. Therefore, we can not proclaim acceptance of three groups by using this statistical method.

Since the number of GRBs is low for many bins, we also used the maximum likelihood method (see Horváth 2002 and the references therein) in order to fit two and three log-normal functions on the RHESSI data-set.

The parameters are listed in the Table 3.

As the difference of the logarithms of the likelihoods $\Delta \ln L = 9.2$ should be half of the χ^2 distribution for 3 degrees of freedom (Horváth 2002), we obtain that the introduction of a third group is statistically significant on the 0.036 % level (of being accidental).

To get an image how T_{90} uncertainties effect our result, we proceed similarly as in the χ^2 fitting and generated ten different data-sets randomly changed in durations by the full amount of their uncertainties. The results are presented in the Table 4. From this table it is seen that all ten simulations give probabilities, that introducing of the third group is accidental, much lower than 5 %. Thus, the hypothesis of introducing third group is highly acceptable.

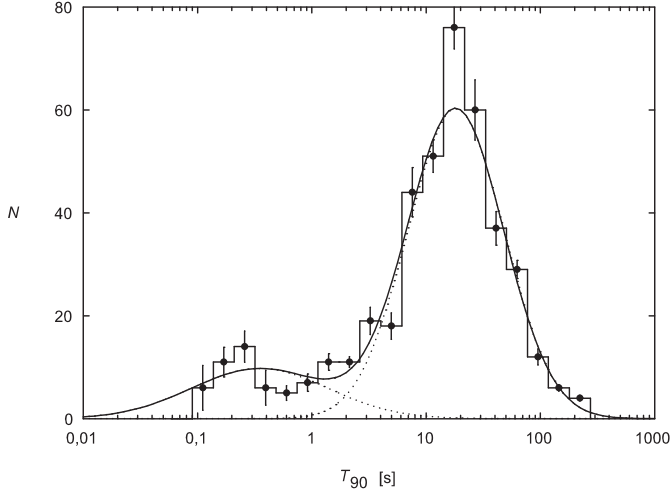


Fig. 1. Duration distribution of the 427 RHESSI bursts with the best χ^2 fit of two log-normal functions. Number of bins is 19, $dof = 14$ and $\chi^2 \approx 19.1$ which implies the goodness-of-fit $\approx 16\%$. The bar errors are standard deviations of the number of GRBs per bin for ten different simulated duration distributions as described in the text.

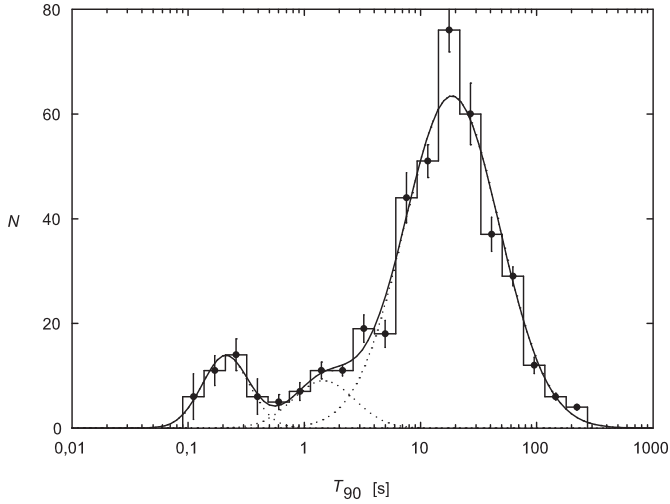


Fig. 2. Duration distribution of the 427 RHESSI bursts with the best χ^2 fit of three log-normal functions. Number of bins is 19, $dof = 11$ and $\chi^2 \approx 10.3$ which implies the goodness-of-fit $\approx 50\%$. The bar errors are the same as described in Fig. 1.

4. Hardness Ratio vs. Duration

A two-dimensional scatter plot of RHESSI GRBs is shown in Fig. 3 and Fig. 4. One axis is the duration T_{90} , used in the previous section, the other axis is a hardness ratio. The hardness ratio is defined as a ratio of two fluences F in two different energy bands integrated over the time interval T_{90} . For the RHESSI data-set, we used the energy bands (25 – 120) keV and (120 – 1500) keV, i.e. $H = F_{120-1500}/F_{25-120}$.

Using the maximum likelihood method (see Horváth et al. (2004), Horváth et al. (2006) and the references therein), we fit two and three bivariate log-normal functions in order to search

Table 1. Parameters of the best χ^2 fits of two and three log-normal functions on the RHESSI GRB T_{90} distribution. μ are the means, σ are the standard deviations and w are the weights of the distribution. Given uncertainties are standard deviations of the parameters obtained by ten different fittings of randomly changed histograms of durations by their uncertainties.

| parameter | 2 log-normal | 3 log-normal |
|--------------------------|------------------|------------------|
| μ_{short} | -0.46 ± 0.13 | -0.68 ± 0.09 |
| σ_{short} | 0.60 ± 0.06 | 0.20 ± 0.03 |
| $w_{\text{short}}[\%]$ | 18.7 ± 1.5 | 8.9 ± 1.0 |
| μ_{long} | 1.26 ± 0.03 | 1.27 ± 0.03 |
| σ_{long} | 0.42 ± 0.01 | 0.41 ± 0.01 |
| $w_{\text{long}}[\%]$ | 81.3 ± 1.5 | 83.4 ± 0.9 |
| μ_{middle} | | 0.17 ± 0.06 |
| σ_{middle} | | 0.27 ± 0.06 |
| $w_{\text{middle}}[\%]$ | | 7.7 ± 1.0 |
| dof | 14 | 11 |
| χ^2 | 19.13 | 10.30 |
| goodness[%] | 16.0 | 50.4 |
| F_0 | 3.14 | |
| $P(F > F_0)[\%]$ | 6.9 | |

Table 2. The minimal χ^2 , corresponding goodness-of-fits and F-tests for fitted two and three log-normal functions on the RHESSI GRB T_{90} distribution for ten different changes of durations by their uncertainties.

| 2 log-normal | | 3 log-normal | | F-test |
|--------------|--------------|--------------|--------------|------------------|
| χ^2 | goodness [%] | χ^2 | goodness [%] | $P(F > F_0)$ [%] |
| 23.97 | 4.6 | 14.19 | 22.3 | 11.1 |
| 18.03 | 20.6 | 10.65 | 47.3 | 11.0 |
| 15.99 | 31.4 | 5.13 | 92.5 | 0.5 |
| 13.52 | 48.6 | 7.50 | 75.8 | 8.0 |
| 17.87 | 21.3 | 7.55 | 75.3 | 2.0 |
| 16.36 | 29.2 | 9.66 | 56.1 | 11.0 |
| 11.89 | 61.5 | 6.95 | 80.3 | 10.4 |
| 21.86 | 8.2 | 13.77 | 24.6 | 15.1 |
| 20.07 | 12.8 | 9.49 | 57.7 | 3.5 |
| 20.40 | 11.8 | 12.73 | 31.1 | 14.4 |

for clusters. In Fig. 3., we show the best fit of two bivariate log-normal functions (11 independent parameters, since the two weights must add up to 100%).

The parameters are listed in Table 5. One result is that the short GRBs are on average harder than long GRBs. Having a closer look at the GRB distribution within the short class, one can see that the points within the 1σ ellipse are not evenly distributed. They cluster towards the shortest durations (Fig. 3).

The fitting with the sum of three groups (17 independent parameters) is shown in Fig. 4. The fitted parameters are listed in Table 5. The former short group is clearly separated into two parts. As far as one can tell by sight, the data points scatter evenly within (and around) the 1σ ellipses.

As the difference of the logarithms of the likelihoods $\Delta \ln L = 10.9$ should be half of the χ^2 distribution for 6 degrees

Table 3. Parameters of the best fit with two and three log-normal functions done by the maximum likelihood method on the RHESSI data. μ are the means, σ are the standard deviations, w are the weights of the distribution and L_2, L_3 are the likelihoods. Given uncertainties are standard deviations of the parameters obtained by ten different fittings of data-sets, in which the durations were randomly changed by their uncertainties.

| parameter | 2 log-normal | 3 log-normal |
|--------------------------|------------------|------------------|
| μ_{short} | -0.60 ± 0.07 | -0.64 ± 0.02 |
| σ_{short} | 0.25 ± 0.05 | 0.20 ± 0.02 |
| $w_{\text{short}}[\%]$ | 10.2 ± 1.3 | 9.4 ± 0.4 |
| μ_{long} | 1.20 ± 0.01 | 1.26 ± 0.01 |
| σ_{long} | 0.47 ± 0.01 | 0.41 ± 0.01 |
| $w_{\text{long}}[\%]$ | 89.8 ± 1.3 | 84.4 ± 1.0 |
| μ_{middle} | | 0.17 ± 0.04 |
| σ_{middle} | | 0.22 ± 0.06 |
| $w_{\text{middle}}[\%]$ | | 6.2 ± 1.4 |
| $\ln L_2$ | -389.17 | |
| $\ln L_3$ | | -379.95 |

Table 4. The maximal likelihoods and corresponding probabilities that introducing of the third group is accidental for maximum likelihood fittings (one-dimensional) with two and three log-normal functions of ten different changes of durations by their uncertainties.

| $\ln L_2$ | $\ln L_3$ | probability [%] |
|-----------|-----------|-----------------|
| -388.12 | -378.86 | 0.03 |
| -390.82 | -383.92 | 0.32 |
| -391.90 | -380.97 | 0.01 |
| -391.75 | -385.37 | 0.52 |
| -392.25 | -384.24 | 0.11 |
| -390.62 | -383.67 | 0.30 |
| -386.26 | -375.54 | 0.01 |
| -392.33 | -384.97 | 0.21 |
| -389.16 | -380.93 | 0.09 |
| -390.21 | -384.32 | 0.82 |

of freedom (Horváth et al. 2006), we obtain that the introduction of a third group is statistically significant on the 0.13% level (of being accidental).

To get an image how GRB durations and hardness ratio uncertainties effect our result, we proceed similarly as in the χ^2 fitting and generated ten different data-sets randomly changed in durations and hardness ratios by the full amount of their uncertainties. The results are presented in the Table 6. From this table it is seen that almost all simulations give probabilities, that introducing of the third group is accidental, much lower than 5%. Thus, the hypothesis of introducing the third group is highly acceptable.

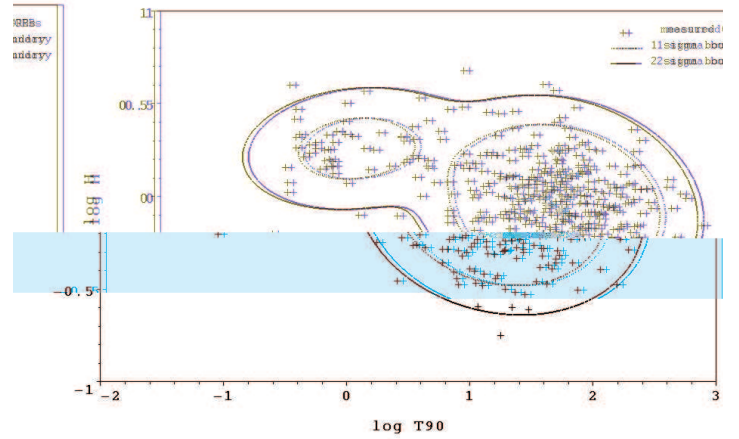


Fig. 3. Hardness ratio vs. T_{90} of the RHESSI GRBs with the best fit of two bivariate log-normal functions.

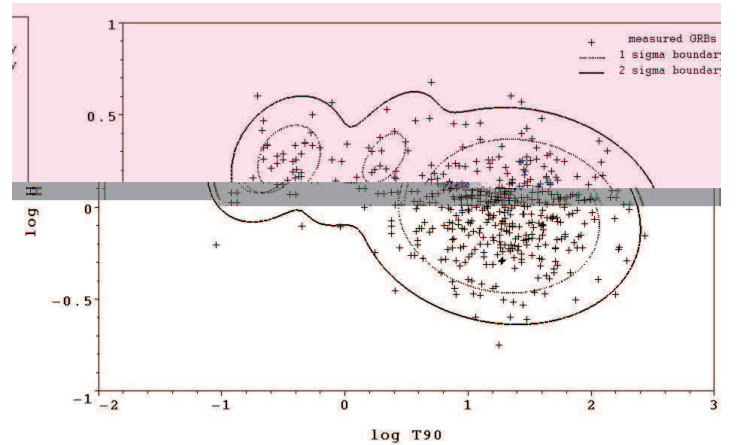


Fig. 4. Hardness ratio vs. T_{90} of the RHESSI GRBs with the best fit of three bivariate log-normal functions.

5. Discussion

The analysis of the 1-dimensional duration distribution, by the χ^2 fitting, reveals the class of so called long GRBs (about 83% of all RHESSI GRBs) with typical durations from 5 to 70 seconds, the most probable duration being $T_{90} \approx 19$ s. Another class are short GRBs (about 9% of all RHESSI GRBs) with typical durations from 0.1 to 0.4 seconds, the most probable duration being $T_{90} \approx 0.21$ s. By fitting 3 log-normal functions we find a third class (about 8% of all RHESSI GRBs) with typical durations from 0.8 to 3 seconds, the most probable duration being $T_{90} \approx 1.5$ s. The existence of the intermediate class from the RHESSI T_{90} distribution is not confirmed on a sufficiently high significance using only the χ^2 fit. However, the maximum likelihood ratio test on the same data reveals that the introduction of a third class is statistically significant. The χ^2 method might not be as much sensitive and hence decisive as the likelihood method, because of the low number of bursts in our data-sample (Horváth et al. 2008, 2nd section, 1st paragraph).

The hardness ratio vs. duration plot for the RHESSI sample does further demonstrate the existence of a third class. The typical durations are very similar to the ones obtained with the 1-dimensional analysis, the percentages are slightly different ($\approx 86\%$ long, $\approx 9\%$ short, $\approx 5\%$ intermediate).

Three classes of GRBs were also reported for the BATSE GRBs (Horváth et al. 2006) and the Swift GRBs

Table 5. Parameters of the best fit with two and three bivariate log-normal functions done by the maximum likelihood method on the RHESSI data. μ_x are the means on the x -axis ($x = \log T_{90}$), μ_y are the means on the y -axis ($y = \log H$), σ_x are the dispersions on the x -axis, σ_y are the dispersions on the y -axis, r are the correlation coefficients, w are the weights of the distribution and L_2, L_3 are the likelihoods. Given uncertainties are standard deviations of the parameters obtained by ten different fittings of data-sets, where the durations and hardness ratios were randomly changed by their uncertainties.

| parameter | 2 log-normal | 3 log-normal |
|---------------------|-------------------|-------------------|
| $\mu_{x,short}$ | -0.38 ± 0.018 | -0.65 ± 0.018 |
| $\mu_{y,short}$ | 0.26 ± 0.010 | 0.26 ± 0.009 |
| $\sigma_{x,short}$ | 0.42 ± 0.012 | 0.20 ± 0.016 |
| $\sigma_{y,short}$ | 0.15 ± 0.009 | 0.15 ± 0.012 |
| $w_{short}[\%]$ | 14.2 ± 0.3 | 9.2 ± 0.5 |
| r_{short} | 0.14 ± 0.092 | 0.22 ± 0.119 |
| $\mu_{x,long}$ | 1.25 ± 0.004 | 1.25 ± 0.006 |
| $\mu_{y,long}$ | -0.05 ± 0.004 | -0.05 ± 0.004 |
| $\sigma_{x,long}$ | 0.42 ± 0.004 | 0.42 ± 0.005 |
| $\sigma_{y,long}$ | 0.22 ± 0.003 | 0.22 ± 0.003 |
| $w_{long}[\%]$ | 85.8 ± 0.3 | 85.5 ± 0.8 |
| r_{long} | -0.14 ± 0.018 | -0.13 ± 0.020 |
| $\mu_{x,middle}$ | | 0.11 ± 0.029 |
| $\mu_{y,middle}$ | | 0.27 ± 0.019 |
| $\sigma_{x,middle}$ | | 0.21 ± 0.057 |
| $\sigma_{y,middle}$ | | 0.17 ± 0.035 |
| $w_{middle}[\%]$ | | 5.3 ± 1.1 |
| r_{middle} | | 0.59 ± 0.230 |
| $\ln L_2$ | -323.91 | |
| $\ln L_3$ | | -313.00 |

Table 6. The maximal likelihoods and corresponding probabilities that introducing of the third group is accidental for maximum likelihood fittings (two-dimensional) with two and three bivariate log-normal functions of ten different changes of durations and hardness ratios by their uncertainties.

| $\ln L_2$ | $\ln L_3$ | probability [%] |
|-----------|-----------|--------------------|
| -349.40 | -339.92 | 0.42 |
| -348.28 | -336.36 | 0.06 |
| -350.66 | -340.80 | 0.31 |
| -347.12 | -338.15 | 0.64 |
| -349.64 | -340.47 | 0.54 |
| -344.59 | -338.17 | 4.56 |
| -350.36 | -342.47 | 1.50 |
| -344.44 | -334.71 | 0.35 |
| -349.37 | -336.51 | 0.03 |
| -348.06 | -338.57 | 0.42 |

(Horváth et al. 2008). For BATSE, $\approx 65\%$ of all GRBs are long, $\approx 24\%$ short and $\approx 11\%$ intermediate (Horváth et al. 2006 Table 2. of that article). The typical durations found for BATSE are roughly a factor 2 longer than for RHESSI, but consistent for all three classes. As is known from BATSE, also in the RHESSI

data-set, the short GRBs are on average harder than the long GRBs. The most remarkable difference is the hardness of the intermediate class. In the BATSE data, the intermediate class has the lowest hardness ratio, which is anti-correlated with the duration (Horváth et al. 2006), whereas we find for the RHESSI data that its hardness is comparable with that of the short group and correlated with the duration, but this correlation is not conclusive because of its large error. The hardness of the intermediate class found with RHESSI is surprising since the intermediate class in the BATSE data was found to be the softest. This discrepancy might be explained by the different definitions of the hardnesses. The hardness H for the RHESSI data is defined as $H = F_{120-1500}/F_{25-120}$, whereas for the BATSE data $H = F_{100-320}/F_{50-100}$, where the numbers denotes energy in keV (the BATSE fluences at higher energies than 320 keV are noisy (Bagoly et al. 1998)). This means that hardnesses do not measure the same bursts' behaviours. Even more different is the situation if we compare hardnesses in the Swift and RHESSI databases, because the Swifts' hardnesses are defined as $H = F_{100-150}/F_{50-100}$ and $H = F_{50-100}/F_{25-50}$ (Horváth et al. 2008, Sakamoto et al. 2008).

The shorter durations of the RHESSI GRBs compared to the BATSE GRBs can be understood: For RHESSI, which is practically unshielded, the background is high (minimum around 1000 counts per second in the (25 – 1500) keV band) and varies by up to a factor 3. Additionally, RHESSI's sensitivity drops rapidly below ≈ 50 keV. Weak GRBs (in the sense of counts per second) and soft GRBs are not so well observed by RHESSI. Since GRBs tend to be softer and weaker at later times, they will sooner fall beyond RHESSI's detection limit, resulting in a shorter duration.

For Swift, $\approx 58\%$ of all GRBs are long, $\approx 7\%$ short and $\approx 35\%$ intermediate (Horváth et al. 2008). The percentage of each group depends obviously on the instrument.

6. Conclusion

The RHESSI data confirm that GRBs can be separated into a short and long class, and that the short GRBs are on average harder than the long ones. The two-dimensional analysis in the hardness/duration plane as well as the maximum likelihood fit of the duration distribution show a third class with intermediate duration and similar hardness as the short class.

Acknowledgements. This study was supported by the GAUK grant No. 46307, by the OTKA grants No. T48870 and K 77795, by the Grant Agency of the Czech Republic grant No. 205/08/H005, by the Research Program MSM0021620860 of the Ministry of Education of the Czech Republic, by the INTEGRAL PECS Project 98023 and by the grant GA ČR 205/08/1207. We appreciate help of K. Hurley with the RHESSI GRB list, valuable discussion with L.G. Balázs and useful remarks of O. Wigger. Thanks are due to the anonymous referee for the worthwhile notes.

References

- Aptekar, R.L., et al. 1998, AIPC, 428, 10
- Band, D.L., et al. 1997, ApJ, 485, 747, Appendix A
- Bagoly, Z., et al. 1998, ApJ, 498, 342
- Chattopadhyay, T., et al. 2007, ApJ, 667, 1017
- Freeland, S.L., et al. 2008, <http://www.lmsal.com/solarsoft>
- Hakkila, J., et al. 2000, ApJ, 538, 165
- Hakkila, J., et al. 2004, Baltic Astronomy, 13, 211
- Holman, G.D. 2008, <http://hesperia.gsfc.nasa.gov/hessi>
- Horváth, I. 1998, ApJ, 508, 757
- Horváth, I. 2002, A&A, 392, 791
- Horváth, I., et al. 2004, Baltic Astronomy, 13, 217
- Horváth, I., et al. 2006, A&A, 447, 23
- Horváth, I., et al. 2008, A&A, 489, L1

Hurley, K. 2007, <http://www.ssl.berkeley.edu/ipn3/index.html>
 Hurley, K. 2008, <http://www.ssl.berkeley.edu/ipn3/masterli.html>
 Kouveliotou, C., et al. 1993, *ApJ*, 413, 101
 Lin, R.P., et al. 2002, *Solar Physics*, 210, 3
 Meegan, C.A., et al. 2001, *Current BATSE Gamma-Ray Burst Catalog*, <http://gammaray.msfc.nasa.gov/batse/grb/catalog>
 Mukherjee, S., et al. 1998, *ApJ*, 508, 314
 Press, W.H., et al. 1992, *Numerical Recipes in C*, Cambridge University Press
 RSI IDL, <http://rsinc.com/idl/>
 Sakamoto, T., et al. 2008, *ApJS*, 175, 179
 Smith, D.M., et al. 2002, *Solar Physics*, 210, 33
 Smith, D.M., et al. 2003, *Proceedings of SPIE Vol. 4851*, 1163
 Trumpler, R.J. & Weaver, H.F. 1953, *Statistical Astronomy*, University of California Press, Berkeley
 Wigger, C., et al. 2006, http://grb.web.psi.ch/publications/talk_venice.pdf
 Wigger, C., et al. 2006, *Il Nuovo Cimento*, 121 B, N. 10-11, 1117
 Wigger, C., et al. 2008, <http://grb.web.psi.ch>
 Zey, C, et al. NIST/SEMATECH, *e-Handbook of Statistical Methods*, <http://www.itl.nist.gov/div898/handbook/>, 2006

Table 7. The RHESSI GRB data-set including I. GRB names which correspond to dates (the letters after GRB names are internal and do not have to be in accordance with e.g. GCN GRB names), II. GRB peak time, III. T_{90} duration, IV. time resolution δt_{res} (described above) and V. hardness ratios.

| GRB | peak time UTC | T_{90} [s] | δt_{res} [s] | hardness ratio $\log H$ |
|---------|------------------|-----------------|-------------------------|----------------------------|
| 020214 | 18:49:47.700 | (1.42±0.03)E+1 | 2.0E-1 | (6.03±0.16)E-1 |
| 020218 | 19:49:41.750 | (3.40±0.06)E+1 | 5.0E-1 | -(1.12±0.11)E-1 |
| 020302 | 12:23:54.400 | (4.88±0.32)E+1 | 8.0E-1 | (1.65±0.53)E-1 |
| 020306 | 18:58:02.893 | (1.35±0.16)E-1 | 1.5E-2 | (4.16±0.40)E-1 |
| 020311 | 01:21:31.550 | (1.08±0.06)E+1 | 3.0E-1 | (6.55±3.88)E-2 |
| 020313 | 01:17:53.400 | (2.32±0.10)E+1 | 4.0E-1 | -(5.17±0.50)E-1 |
| 020315 | 15:42:47.550 | (1.26±0.11)E+1 | 3.0E-1 | (2.97±6.94)E-2 |
| 020331 | 10:23:26.750 | (3.90±0.53)E+1 | 5.0E-1 | -(0.46±1.05)E-1 |
| 020407 | 04:14:44.300 | (2.10±0.09)E+1 | 6.0E-1 | -(1.72±2.76)E-2 |
| 020409 | 09:27:23.500 | (1.46±0.14)E+2 | 1.0E+0 | (8.84±7.37)E-2 |
| 020413 | 16:20:15.500 | (9.00±0.64)E+0 | 2.0E-1 | -(2.89±5.57)E-2 |
| 020417 | 05:36:26.250 | (7.85±0.52)E+1 | 5.0E-1 | -(1.62±0.58)E-1 |
| 020418 | 17:43:08.850 | (3.40±0.13)E+0 | 1.0E-1 | (1.81±0.20)E-1 |
| 020426 | 23:56:14.795 | (1.20±0.32)E-1 | 3.0E-2 | (7.40±7.13)E-2 |
| 020430 | 21:22:01.650 | (1.35±0.05)E+1 | 3.0E-1 | -(2.73±0.32)E-1 |
| 020509 | 00:01:17.675 | (3.50±0.38)E+0 | 5.0E-2 | (8.32±8.52)E-2 |
| 020524 | 02:12:47.300 | (1.48±0.08)E+1 | 2.0E-1 | (7.46±4.26)E-2 |
| 020525A | 03:47:53.650 | (7.60±0.61)E+0 | 1.0E-1 | (1.10±0.65)E-1 |
| 020525B | 04:26:53.210 | (1.80±0.29)E-1 | 2.0E-2 | (2.78±0.96)E-1 |
| 020527 | 05:17:20.525 | (1.65±0.18)E+0 | 5.0E-2 | (1.94±0.88)E-1 |
| 020602 | 17:30:28.085 | (1.75±0.19)E+0 | 7.0E-2 | -(2.49±0.91)E-1 |
| 020603 | 17:50:34.905 | (1.44±0.06)E+0 | 3.0E-2 | -(0.07±3.08)E-2 |
| 020604 | 14:13:42.850 | (7.20±0.41)E+0 | 3.0E-1 | -(1.37±3.19)E-2 |
| 020620 | 12:58:06.875 | (3.45±0.22)E+0 | 5.0E-2 | -(2.63±0.56)E-1 |
| 020623 | 04:23:07.350 | (6.60±0.46)E+0 | 1.0E-1 | -(2.84±0.66)E-1 |
| 020630 | 07:58:52.650 | (3.30±0.26)E+1 | 3.0E-1 | -(1.48±0.66)E-1 |
| 020702 | 15:54:16.250 | (3.69±0.24)E+1 | 3.0E-1 | -(3.85±0.71)E-1 |
| 020708 | 04:34:12.500 | (2.70±0.40)E+1 | 1.0E+0 | -(3.00±1.29)E-1 |
| 020712 | 06:09:44.100 | (1.80±0.20)E+1 | 2.0E-1 | -(1.51±0.93)E-1 |
| 020715A | 15:14:26.735 | (2.40±0.40)E-1 | 3.0E-2 | (1.92±0.88)E-1 |
| 020715B | 19:21:09.100 | (6.40±0.21)E+0 | 2.0E-1 | (1.05±0.10)E-1 |
| 020725 | 16:25:41.150 | (5.00±0.31)E+0 | 1.0E-1 | (2.37±0.51)E-1 |
| 020801 | 11:52:41.550 | (1.43±0.09)E+1 | 1.0E-1 | -(8.54±5.30)E-2 |
| 020819A | 07:56:39.455 | (1.05±0.08)E+0 | 3.0E-2 | (1.85±0.60)E-1 |
| 020819B | 14:57:38.600 | (9.20±0.75)E+0 | 4.0E-1 | -(2.13±0.64)E-1 |
| 020828 | 05:45:37.925 | (6.60±0.45)E-1 | 3.0E-2 | (3.41±0.48)E-1 |
| 020910 | 19:57:43.150 | (2.85±0.10)E+1 | 3.0E-1 | (1.33±0.29)E-1 |
| 020914 | 21:53:20.100 | (1.08±0.09)E+1 | 2.0E-1 | -(2.54±0.73)E-1 |
| 020926 | 04:52:54.200 | (2.24±0.15)E+1 | 8.0E-1 | -(2.05±0.53)E-1 |
| 021008A | 07:01:03.550 | (1.45±0.01)E+1 | 1.0E-1 | (1.34±0.03)E-1 |
| 021008B | 14:30:04.500 | (1.42±0.12)E+1 | 2.0E-1 | (0.09±6.92)E-2 |
| 021011 | 04:38:11.250 | (5.10±0.32)E+1 | 5.0E-1 | -(2.94±0.61)E-1 |
| 021016 | 10:29:43.500 | (8.30±0.54)E+1 | 1.0E+0 | -(1.54±0.55)E-1 |
| 021020 | 20:12:57.350 | (1.44±0.04)E+1 | 3.0E-1 | -(0.64±1.86)E-2 |
| 021023 | 02:53:47.300 | (1.36±0.05)E+1 | 2.0E-1 | -(0.60±2.85)E-2 |
| 021025 | 20:18:30.150 | (1.86±0.22)E+1 | 3.0E-1 | -(1.22±0.95)E-1 |
| 021102 | 15:58:31.850 | (1.08±0.05)E+1 | 3.0E-1 | -(4.04±0.41)E-1 |
| 021105 | 05:27:18.650 | (6.40±0.80)E+0 | 1.0E-1 | -(9.92±9.89)E-2 |
| 021108 | 05:39:55.800 | (2.20±0.17)E+1 | 4.0E-1 | -(5.99±1.07)E-1 |
| 021109 | 08:42:49.000 | (1.96±0.13)E+1 | 4.0E-1 | -(2.87±5.23)E-2 |
| 021113 | 13:37:37.625 | (3.98±0.48)E+1 | 2.5E-1 | -(2.82±1.08)E-1 |
| 021115 | 13:33:04.250 | (1.26±0.15)E+1 | 3.0E-1 | -(4.79±1.31)E-1 |
| 021119 | 12:54:07.700 | (2.82±0.08)E+1 | 2.0E-1 | -(1.83±0.26)E-1 |
| 021125 | 17:58:31.250 | (6.75±0.12)E+1 | 5.0E-1 | -(3.57±0.18)E-1 |
| 021201 | 05:30:04.175 | (3.40±0.16)E-1 | 1.0E-2 | (4.03±0.36)E-1 |
| 021205 | 03:18:29.750 | (7.65±0.33)E+1 | 1.5E+0 | -(2.23±0.36)E-1 |
| 021206 | 22:49:16.650 | (4.92±0.02)E+0 | 2.0E-2 | (2.26±0.22)E-2 |
| 021211 | 11:18:35.040 | (4.32±0.32)E+0 | 8.0E-2 | -(2.79±0.68)E-1 |
| 021214 | 03:27:25.500 | (3.00±0.28)E+1 | 1.0E+0 | -(2.07±0.77)E-1 |
| 021223 | 01:10:00.250 | (8.00±0.64)E+0 | 1.0E-1 | -(2.92±0.77)E-1 |
| 021226 | 14:53:39.675 | (3.50±0.53)E-1 | 5.0E-2 | (3.34±0.43)E-1 |
| 030102 | 23:18:59.350 | (1.32±0.09)E+1 | 3.0E-1 | -(1.65±0.56)E-1 |

Table 12. The RHESSI GRB data-set.

| GRB | peak time UTC | T_{90} [s] | δt_{res} [s] | hardness ratio log H |
|---------|------------------|-----------------|-------------------------|---------------------------|
| 060313 | 20:11:32.900 | (3.60±0.51)E+0 | 2.0E-1 | (1.52±1.03)E-1 |
| 060323 | 07:04:30.100 | (1.76±0.04)E+1 | 2.0E-1 | (3.37±1.52)E-2 |
| 060325 | 12:02:20.350 | (1.08±0.02)E+1 | 1.0E-1 | (0.70±1.11)E-2 |
| 060401 | 05:40:18.750 | (6.30±0.17)E+0 | 1.0E-1 | (9.21±1.86)E-2 |
| 060408 | 13:11:39.150 | (6.90±0.95)E+0 | 3.0E-1 | (-0.06±1.01)E-1 |
| 060415 | 05:31:00.050 | (1.32±0.20)E+1 | 3.0E-1 | (1.80±1.14)E-1 |
| 060418 | 03:06:35.800 | (4.08±0.21)E+1 | 4.0E-1 | (-1.23±0.43)E-1 |
| 060421A | 11:03:49.000 | (3.12±0.11)E+1 | 4.0E-1 | (-8.58±2.76)E-2 |
| 060421B | 20:36:38.200 | (2.16±0.19)E+1 | 4.0E-1 | (-1.39±0.74)E-1 |
| 060425 | 16:57:38.705 | (1.40±0.12)E-1 | 1.0E-2 | (-2.59±0.42)E-1 |
| 060428 | 02:30:41.750 | (1.35±0.23)E+1 | 5.0E-1 | (-2.45±1.44)E-1 |
| 060429 | 12:19:51.250 | (2.00±0.21)E-1 | 2.0E-2 | (2.89±0.33)E-1 |
| 060505 | 23:32:01.050 | (9.60±0.46)E+0 | 3.0E-1 | (2.15±0.30)E-1 |
| 060528 | 22:53:05.750 | (7.70±0.20)E+1 | 5.0E-1 | (2.41±0.21)E-1 |
| 060530 | 19:19:11.300 | (4.00±0.35)E+0 | 2.0E-1 | (-1.39±0.63)E-1 |
| 060610 | 11:22:24.070 | (6.00±0.33)E-1 | 2.0E-2 | (2.48±0.38)E-1 |
| 060614 | 12:43:48.250 | (5.25±0.45)E+1 | 1.5E+0 | (-1.78±0.72)E-1 |
| 060622 | 17:19:48.750 | (2.35±0.09)E+1 | 5.0E-1 | (1.12±0.27)E-1 |
| 060624 | 13:46:56.255 | (2.55±0.07)E+0 | 3.0E-2 | (-4.55±0.29)E-1 |
| 060625 | 07:33:27.100 | (4.40±0.37)E+0 | 2.0E-1 | (2.21±0.58)E-1 |
| 060630 | 00:06:41.250 | (4.10±0.19)E+1 | 5.0E-1 | (-9.96±4.00)E-2 |
| 060708 | 04:30:38.485 | (1.14±0.08)E-1 | 6.0E-3 | (1.57±0.36)E-1 |
| 060729 | 04:07:38.600 | (5.20±0.53)E+0 | 2.0E-1 | (-1.16±0.79)E-1 |
| 060805 | 14:27:17.450 | (5.10±0.07)E+0 | 6.0E-2 | (6.98±0.69)E-2 |
| 060811 | 16:56:43.950 | (7.29±0.27)E+1 | 3.0E-1 | (-1.96±0.35)E-1 |
| 060819 | 18:28:20.700 | (2.40±0.11)E+1 | 6.0E-1 | (0.84±3.26)E-2 |
| 060823 | 08:05:33.750 | (1.00±0.18)E+0 | 1.0E-1 | (3.23±1.26)E-1 |
| 060919 | 21:52:12.750 | (2.95±0.37)E+1 | 5.0E-1 | (1.20±0.95)E-1 |
| 060920 | 15:32:38.700 | (2.18±0.03)E+1 | 2.0E-1 | (3.59±1.01)E-2 |
| 060925 | 20:14:35.375 | (1.65±0.08)E+1 | 2.5E-1 | (-1.00±0.38)E-1 |
| 060928 | 01:20:24.150 | (2.03±0.03)E+2 | 3.0E-1 | (-1.28±1.19)E-2 |
| 061005 | 13:38:01.800 | (4.24±0.12)E+1 | 4.0E-1 | (-2.05±0.25)E-1 |
| 061006A | 08:43:39.225 | (1.65±0.10)E+0 | 5.0E-2 | (1.53±0.43)E-1 |
| 061006B | 16:45:27.875 | (4.00±0.53)E-1 | 5.0E-2 | (3.23±0.39)E-1 |
| 061007 | 10:08:54.150 | (6.06±0.07)E+1 | 3.0E-1 | (1.20±0.08)E-1 |
| 061012 | 11:51:57.850 | (9.30±0.48)E+0 | 1.0E-1 | (2.56±0.44)E-1 |
| 061013 | 18:06:28.200 | (4.00±0.22)E+1 | 8.0E-1 | (-1.54±0.45)E-1 |
| 061014 | 06:17:02.375 | (2.00±0.55)E-1 | 5.0E-2 | (2.56±0.94)E-1 |
| 061022 | 12:23:42.850 | (2.19±0.29)E+1 | 3.0E-1 | (-0.44±1.02)E-1 |
| 061031 | 12:19:51.500 | (3.30±0.12)E+1 | 2.0E-1 | (7.92±3.06)E-2 |
| 061101 | 21:26:51.550 | (1.92±0.30)E+1 | 3.0E-1 | (-2.41±1.40)E-1 |
| 061108 | 01:09:54.850 | (3.75±0.09)E+1 | 3.0E-1 | (-8.68±1.90)E-2 |
| 061113 | 13:43:36.050 | (1.82±0.03)E+1 | 1.0E-1 | (1.76±0.13)E-1 |
| 061117 | 06:00:11.250 | (2.15±0.27)E+1 | 5.0E-1 | (9.86±9.49)E-2 |
| 061121 | 15:23:44.275 | (1.46±0.03)E+1 | 1.5E-1 | (1.27±0.17)E-1 |
| 061123 | 16:33:28.650 | (5.70±0.32)E+0 | 1.0E-1 | (1.23±0.43)E-1 |
| 061126 | 08:48:03.150 | (1.65±0.07)E+1 | 3.0E-1 | (2.49±0.31)E-1 |
| 061128 | 20:01:11.805 | (3.00±0.31)E-1 | 3.0E-2 | (3.50±0.27)E-1 |
| 061205 | 05:22:15.450 | (7.50±0.91)E+0 | 3.0E-1 | (-1.22±0.96)E-1 |
| 061212 | 05:31:30.970 | (1.90±0.01)E+1 | 6.0E-2 | (2.73±0.06)E-1 |
| 061222 | 03:30:19.300 | (1.16±0.05)E+1 | 2.0E-1 | (1.44±0.31)E-1 |
| 061229 | 22:25:44.250 | (7.95±0.97)E+1 | 5.0E-1 | (1.69±0.93)E-1 |
| 061230 | 23:09:31.000 | (2.56±0.19)E+1 | 8.0E-1 | (-1.63±0.60)E-1 |
| 070113 | 11:56:23.815 | (2.70±0.48)E-1 | 3.0E-2 | (1.65±1.04)E-1 |
| 070116 | 14:32:16.125 | (1.65±0.11)E+1 | 2.5E-1 | (3.79±5.24)E-2 |
| 070120 | 10:48:36.250 | (1.85±0.27)E+1 | 5.0E-1 | (1.94±1.07)E-1 |
| 070121 | 10:12:17.000 | (8.80±1.60)E+0 | 8.0E-1 | (0.11±1.19)E-1 |
| 070125 | 07:21:27.250 | (5.67±0.08)E+1 | 3.0E-1 | (5.03±1.12)E-2 |
| 070214 | 22:39:20.850 | (1.77±0.27)E+1 | 3.0E-1 | (1.00±1.11)E-1 |
| 070220 | 04:44:45.300 | (2.14±0.11)E+1 | 2.0E-1 | (4.86±4.03)E-2 |
| 070221 | 21:06:46.500 | (1.02±0.13)E+1 | 2.0E-1 | (-2.28±9.64)E-2 |
| 070307 | 21:15:43.250 | (5.25±0.27)E+1 | 5.0E-1 | (-5.80±4.35)E-2 |
| 070402 | 15:48:39.475 | (8.85±0.56)E+0 | 1.5E-1 | (4.96±4.92)E-2 |
| 070420 | 06:18:18.400 | (6.16±0.36)E+1 | 8.0E-1 | (-1.63±0.51)E-1 |
| 070508 | 04:18:25.050 | (1.31±0.04)E+1 | 1.0E-1 | (-1.71±2.74)E-2 |
| 070516 | 20:41:24.725 | (3.50±0.56)E-1 | 5.0E-2 | (5.01±0.73)E-1 |

Table 13. The RHESSI GRB data-set.

| GRB | peak time UTC | T_{90} [s] | δt_{res} [s] | hardness ratio log H |
|--------|------------------|-----------------|-------------------------|---------------------------|
| 070531 | 11:45:43.500 | (2.60±0.34)E+1 | 1.0E+0 | (-1.08±1.03)E-1 |
| 070614 | 05:05:09.425 | (1.50±0.51)E-1 | 5.0E-2 | (3.35±0.64)E-1 |
| 070622 | 02:25:17.850 | (1.38±0.03)E+1 | 1.0E-1 | (1.23±0.18)E-1 |
| 070626 | 04:08:44.500 | (1.43±0.02)E+2 | 1.0E+0 | (5.00±1.07)E-2 |
| 070710 | 08:22:07.850 | (3.90±0.58)E+0 | 3.0E-1 | (0.94±9.91)E-2 |
| 070717 | 21:50:38.750 | (1.75±0.20)E+1 | 5.0E-1 | (2.50±0.87)E-1 |
| 070722 | 06:00:31.500 | (7.20±0.96)E+0 | 2.0E-1 | (1.02±0.99)E-1 |
| 070724 | 23:25:46.500 | (2.40±0.25)E+1 | 1.0E+0 | (-2.08±0.89)E-1 |
| 070802 | 06:16:19.390 | (3.12±0.25)E+0 | 6.0E-2 | (4.80±0.78)E-1 |
| 070817 | 14:43:42.250 | (8.80±0.71)E+1 | 5.0E-1 | (-9.18±6.84)E-2 |
| 070819 | 10:17:04.750 | (3.30±0.26)E+1 | 5.0E-1 | (3.83±6.10)E-2 |
| 070821 | 12:51:31.750 | (6.75±0.21)E+1 | 5.0E-1 | (6.03±2.47)E-2 |
| 070824 | 20:50:10.425 | (1.30±0.07)E+0 | 5.0E-2 | (1.01±0.29)E-1 |
| 070825 | 01:55:54.250 | (3.42±0.09)E+1 | 3.0E-1 | (1.44±0.19)E-1 |
| 070917 | 09:40:31.250 | (2.31±0.24)E+1 | 3.0E-1 | (3.20±0.85)E-1 |
| 071013 | 08:53:39.475 | (3.65±0.43)E+0 | 5.0E-2 | (3.27±8.94)E-2 |
| 071014 | 03:19:52.450 | (7.80±0.37)E+0 | 1.0E-1 | (4.13±3.71)E-2 |
| 071030 | 08:52:41.900 | (6.00±0.91)E+0 | 2.0E-1 | (2.20±1.14)E-1 |
| 071104 | 11:41:09.525 | (1.47±0.13)E+1 | 1.5E-1 | (-6.66±7.12)E-2 |
| 071204 | 05:58:29.475 | (3.00±0.56)E-1 | 5.0E-2 | (3.46±0.72)E-1 |
| 071217 | 17:03:27.950 | (8.30±0.48)E+0 | 1.0E-1 | (-9.40±4.89)E-2 |
| 080114 | 16:10:22.300 | (7.34±0.07)E+1 | 2.0E-1 | (3.60±0.09)E-1 |
| 080202 | 13:04:37.250 | (3.06±0.39)E+1 | 3.0E-1 | (0.15±9.87)E-2 |
| 080204 | 13:56:34.760 | (4.88±0.23)E+0 | 8.0E-2 | (4.53±0.42)E-1 |
| 080211 | 07:23:46.250 | (2.80±0.08)E+1 | 5.0E-1 | (2.79±0.19)E-1 |
| 080218 | 05:57:28.375 | (1.95±0.15)E+1 | 2.5E-1 | (1.18±0.61)E-1 |
| 080224 | 16:58:51.050 | (5.40±0.29)E+0 | 1.0E-1 | (2.22±0.41)E-1 |
| 080318 | 08:31:45.050 | (1.47±0.16)E+1 | 3.0E-1 | (1.51±0.79)E-1 |
| 080319 | 12:25:56.900 | (1.20±0.06)E+1 | 2.0E-1 | (3.29±0.42)E-1 |
| 080320 | 11:52:02.625 | (3.05±0.08)E+1 | 2.5E-1 | (1.96±0.22)E-1 |
| 080328 | 08:03:14.500 | (8.60±0.62)E+1 | 1.0E+0 | (3.03±0.58)E-1 |
| 080330 | 11:04:33.450 | (3.36±0.09)E+1 | 3.0E-1 | (2.54±0.20)E-1 |
| 080408 | 03:36:23.050 | (1.40±0.11)E+0 | 1.0E-1 | (5.29±0.37)E-1 |
| 080413 | 08:51:12.250 | (7.60±1.20)E+0 | 1.0E-1 | (0.55±1.17)E-1 |
| 080425 | 20:21:47.775 | (2.28±0.32)E+1 | 1.5E-1 | (2.58±1.05)E-1 |